Arabidopsis CSP41 proteins form multimeric complexes that bind and stabilize distinct plastid transcripts

Yafei Qi, Ute Armbruster, Christian Schmitz-Linneweber, Etienne Delannoy, Andeol Falcon de Longevialle, Thilo Rühle, Ian Small, Peter Jahns and Dario Leister

Supplementary material

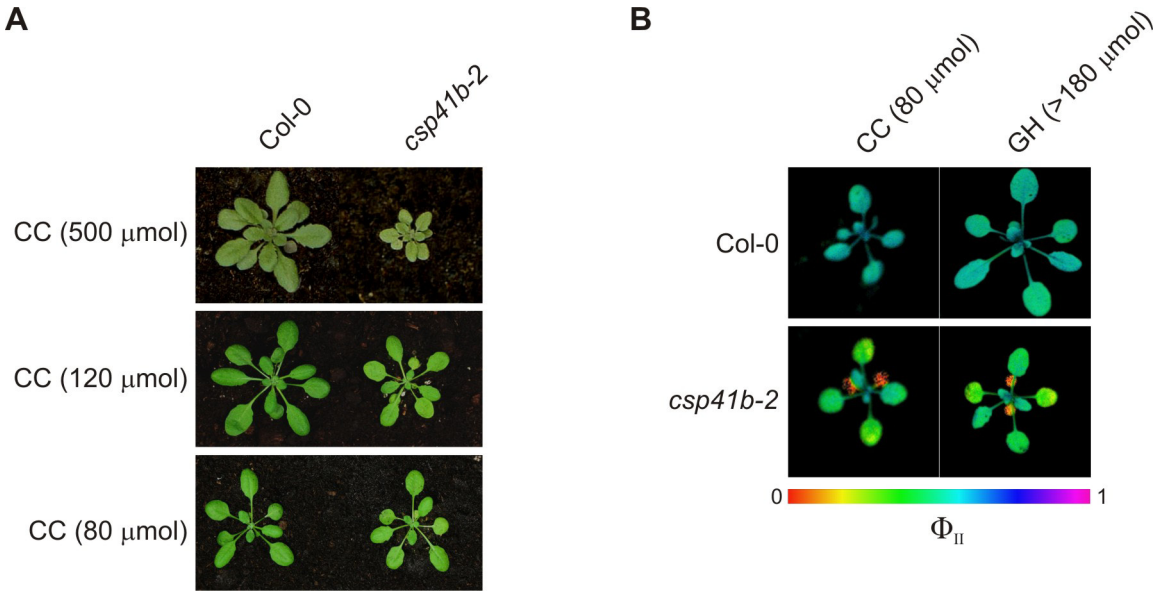

Supplementary Fig. S1. Phenotypical characterization of *csp41* insertion lines.

(A) Phenotypes of 4-week-old WT (Col-0) and *csp41b-2* plants grown in a climate chamber (CC) on a 12 h/12 h light/dark regime at 80 µmol, 120 or 500 µmol photons m^{-2} s^{-1}.

(C) Four-week-old WT (Col-0) and *csp41b-2* plants grown in the climate chamber (80 µmol photons m^{-2} s^{-1}, left panel) an in the greenhouse (right panel) were analyzed for the effective quantum yield of PSII (Φ_{II}) as described in Methods. Signal intensities for Φ_{II} are provided according to the color scale at the bottom of the figure.

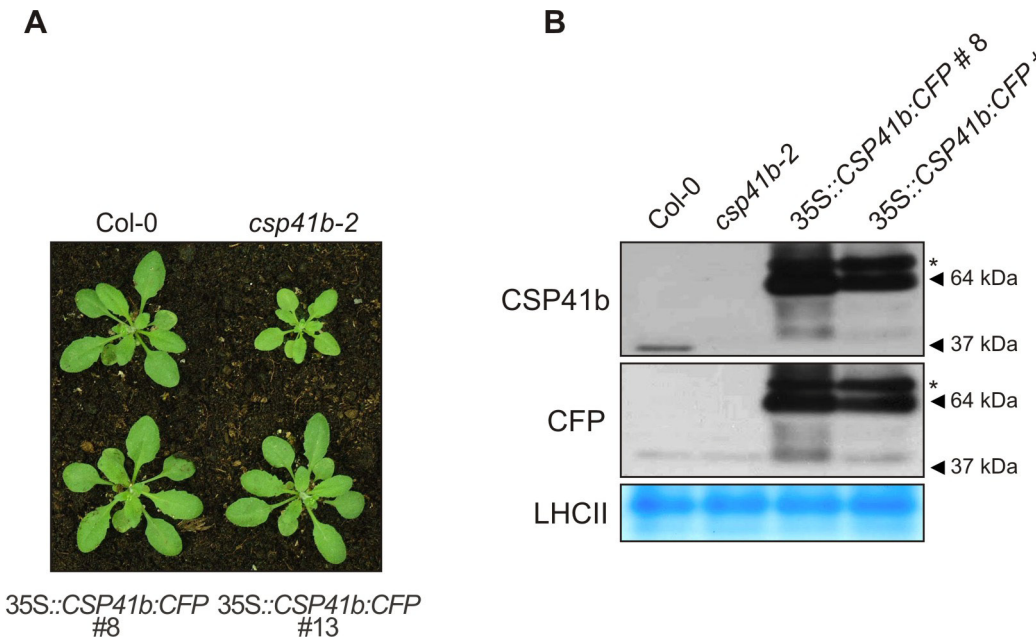

Supplementary Fig. S2. CFP-tagged CSP41b can complement the *csp41b-2* mutation.

(A) Phenotypes of 4-week-old WT (Col-0), *csp41b-2,* and two independent lines resulting from transformation of *csp41b-2* mutant plants with *CSP41b:CFP* under control of the Cauliflower Mosaic Virus 35S promoter (35S*::CSP41b:CFP* #8 and #13).

(B) Immunodetection of the fusion protein in total protein extracts with specific antibodies raised against CSP41b and GFP (Invitrogen). Asterisks indicate a ~70-kDa band that most probably represents the cytoplasmic precursor of the fusion protein. As loading control Coomassie Brilliant Blue (C.B.B.) stained LHCII bands are shown.

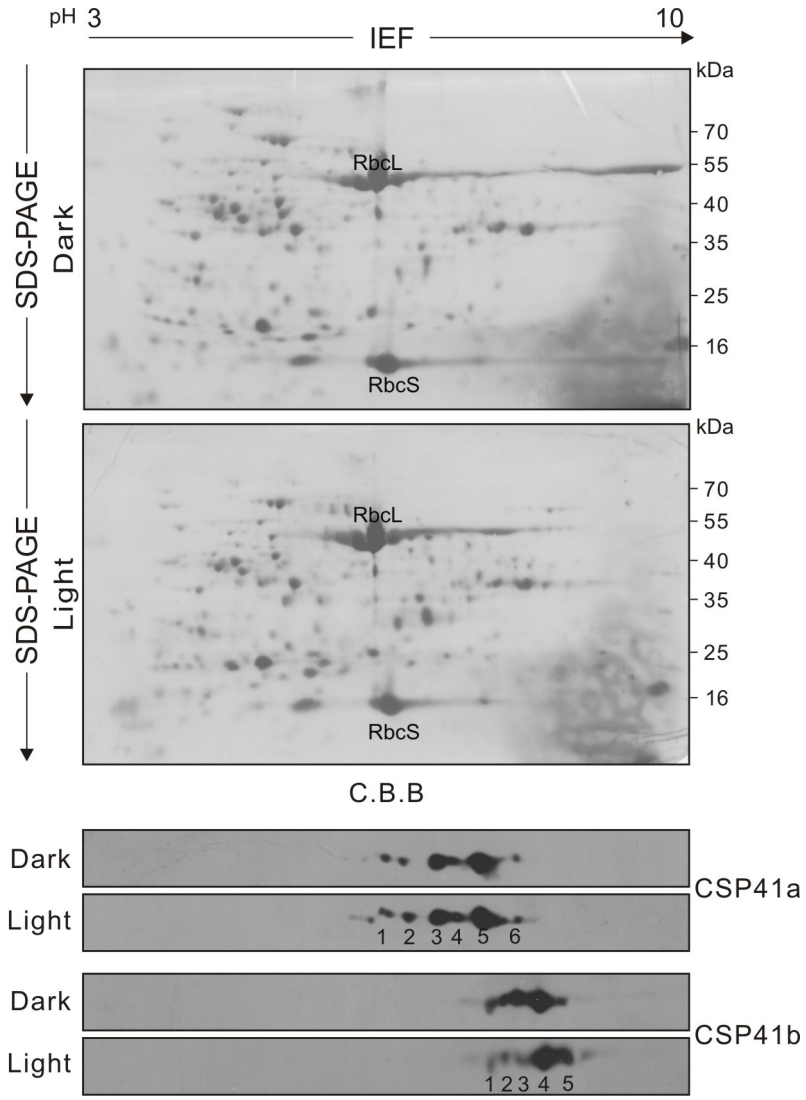

Supplementary Fig. S3. IEF analysis of CSP41b proteins from light- and dark-adapted plants.

Stroma proteins (500 µg) from light- and dark-adapted WT *(Col-0)* plants were fractionated by IEF in the first dimension and by SDS–PAGE in the second. Proteins were transferred to PVDF membranes, stained with Coomassie Brilliant Blue (C.B.B) and immunodecorated with CSP41a- and CSP41b-specific antibodies.

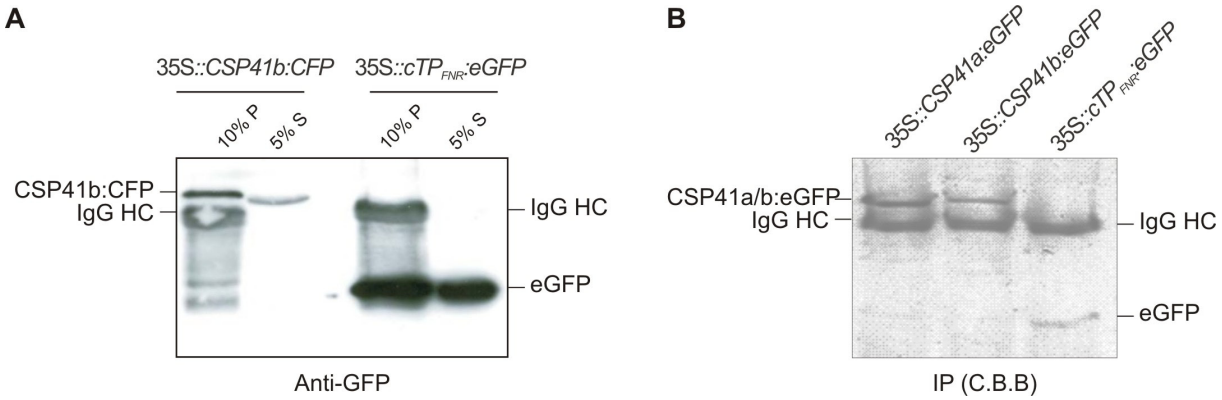

Supplementary Fig. S4. Analysis of immunoprecipitated CFP/eGFP proteins.

(A) Proteins were isolated from pellet and supernatant fractions from immunoprecipitations of CSP41b:CFP and chloroplast localized eGFP (cp-eGFP) as used for RNA extraction for RIP-Chip and slot blot analyses (Fig. 6A-C), fractionated on a 12% SDS-PAGE gel, blotted and labeled with an anti-GFP antibody. Percentages indicate amounts of protein relative to the total volume of pellet (P) and supernatant (S) fractions, respectively, after immunoprecipitation.

(B) Proteins were isolated from the pellet fractions of immunoprecipitated CSP41a:eGFP, CSP41b:eGFP and cp-eGFP as used for RNA extraction for slot-blot analysis (Fig. 6), fractionated on a 12% SDS-PAGE gel and stained with Coomassie Brilliant Blue (C.B.B.).

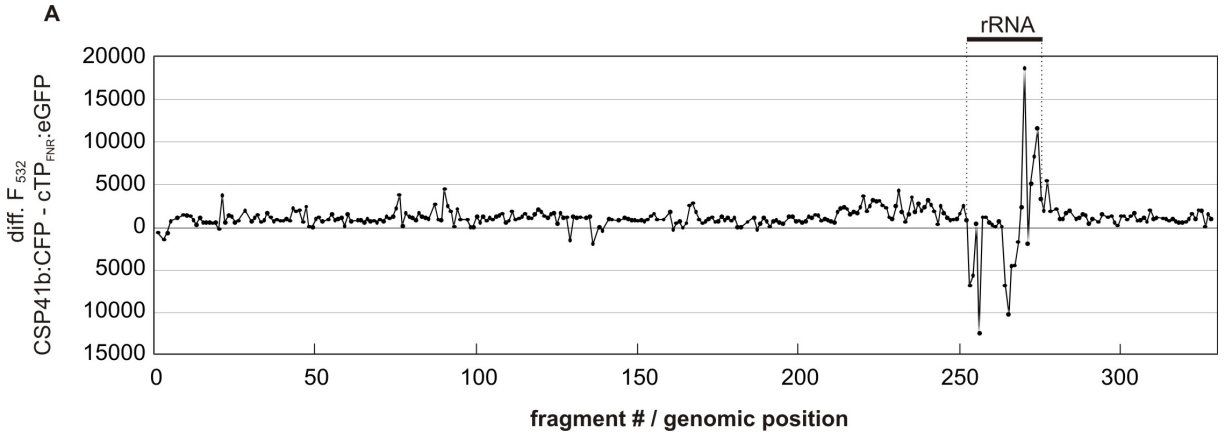

Supplementary Fig. S5. RIP-chip analysis: differential supernatant signals and validation of data.

The experiments described in Figure 6 were used to calculate normalized mean supernatant signals (F_{532}) from cp-eGFP assays, which were then subtracted from those obtained from CSP41b assays. Although there is some variability in signals for PCR products on the array corresponding to ribosomal RNAs (bar), there is no general tendency towards enrichment, and adjacent fragments have very different values for rRNAs. Overall, differences between supernatants from CSP41b:CFP and chloroplast-targeted eGFP (cp-eGFP) immunoprecipitations are minor, and do not coincide with RNAs found to be enriched in CSP41b immunoprecipitation pellets.

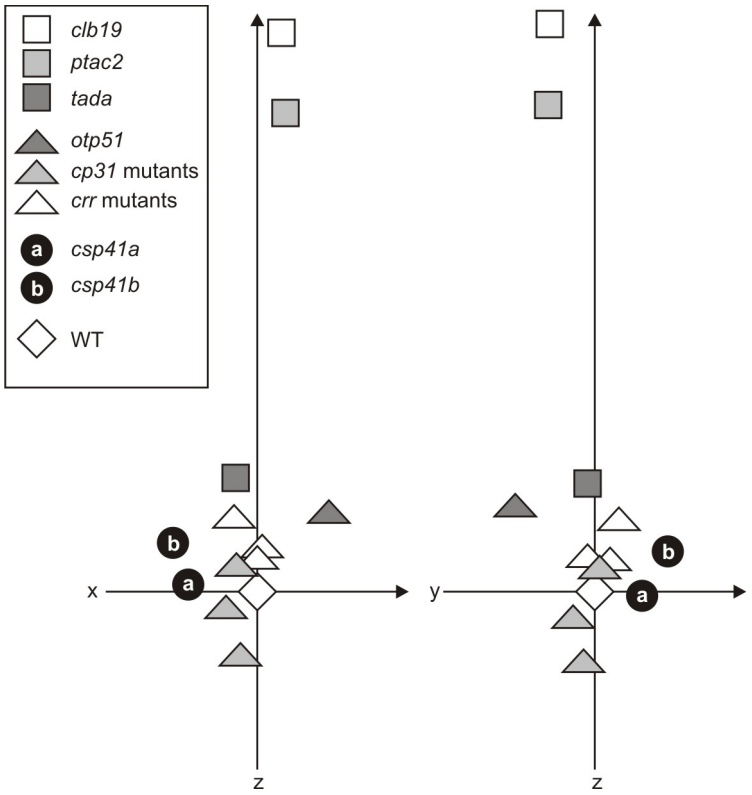

Supplementary Fig. S6. Comparative plastid transcriptome analysis in mutants affecting plastid gene expression.

Principal Component Analysis of mRNA profiles. Levels of plastid RNAs in the *csp41a-4* and *csp41b-2* mutants were quantified by qRT-PCR and compared with those of previously published mutants. The latter class included *crr* mutants impaired in *ndh* transcript maturation steps (Okuda *et al.*, 2007), *otp51* impaired in splicing of some group II introns (de Longevialle *et al.*, 2008), *clb19* and *ptac2* impaired in PEP activity (Chateigner-Boutin *et al.*, 2008), *tada* partially impaired in plastid translation (Delannoy *et al.*, 2009) and *cp31* mutants (Tillich *et al.*, 2009). The profiles for *csp41b*, *csp41a*, *otp51*, *csp31a*, *tada*, *clb19* and *ptac2* are means of at least two biological replicates. Left and right panels show different views of the three-dimensional PCA space rotated by 90° along the vertical axis.

A

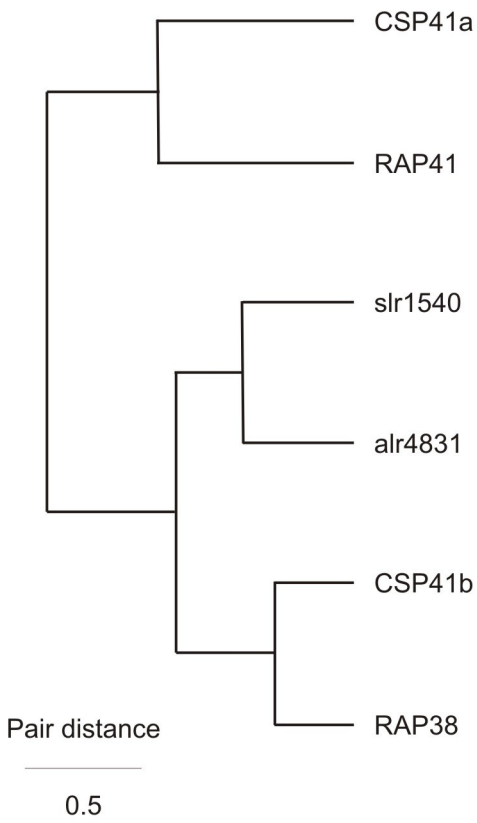
CSP41a
RAP41
slr1540
alr4831
CSP41b
RAP38
Pair distance
0.5

B

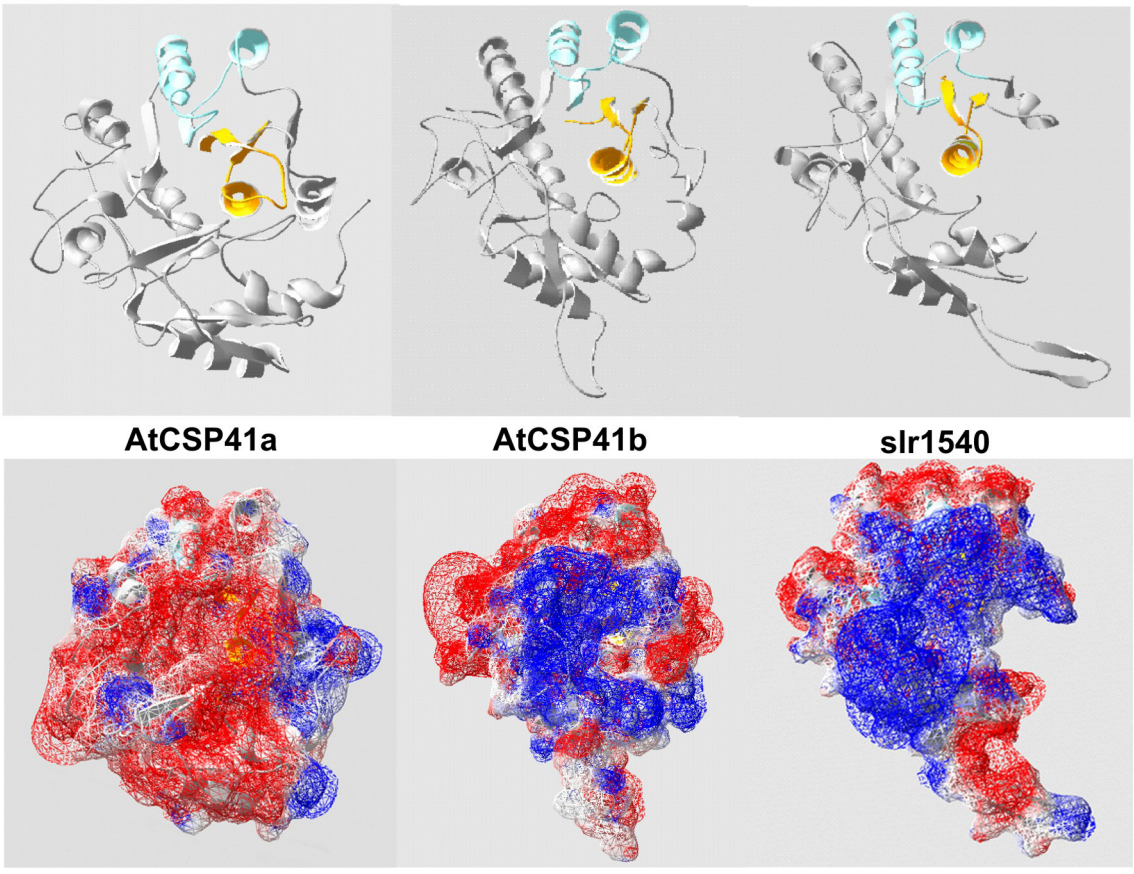
AtCSP41a
AtCSP41b
slr1540

Supplementary Fig. S7. Sequence and structural comparison of CSP41 proteins.

(A) Protein sequences (*Arabidopsis thaliana*, CSP41a and CSP41b; *Chlamydomonas reinhardtii*, RAP41 and RAP38 (Yamaguchi *et al.*, 2003); *Anabaena* sp. PCC 7120, alr_4831; *Synechocystis* sp. PCC 6803, slr1540) were aligned using ClustalW (default settings; gap extensions:1; Thompson *et al.*, 2002). The unrooted phylogram was built using the programs Phylip (version 3.67), Protmlk (default settings; http://evolution.genetics. washington.edu/phylip.html) and Phylodraw (version 0.8; http://pearl.cs. pusan.ac.kr/ phylodraw).

(B) Atom coordinates of mature CSP41a, CSP41b and the cyanobacterial homolog slr1540 were predicted by the 3D-JIGSAW server (version 2.0,www.bmm.icnet.uk/servers/3djigsaw). The three dimensional protein models were visualised using DeepView Swiss-Pdb Viewer (http://expasy. org/spdbv).

Supplemental Table S1. Overview of primers used for amplification of probes for Northern, slot blot, transcription run-on and RNA stability assays.

Gene	sense primer	antisense primer
ndhC	ATGTTTCTGCTTTACGAATATGAT	CTAAGACCATTCCAATGCTCCTT
psaA	GATTATTCGTTCGCCGGAAC	TGGAGCTGCTTTGTGATAATG
rbcL	CGTTGGAGAGACCGTTTCTT	CAAAGCCCAAAGTTGACTCC
psbD	ATGGATGACTGGTTACGGAG	CGAAATATAGCCGCTACACC
psbC	TAGCTTTAGCTGGTCGTGAC	GGTATCATATACGCCCCCAA
rrn23	GAAAGGCTTACGGTGGATAC	ATCGGTCACCCAGGAGTATT
psbE	ATGTCTGGAAGCACAGGAGA	CTAAAAAGATCTACTAAATTCA
rrn16	GCTTAACACATGCAAGTCGG	AAAAAGCCACCTACAGACGC
petD	ATGGGAGTAACAAAAAAACCAG	CCTAGATACCCACGTCGTTT
psbA	TGCATCCGTTGATGAATGGC	CTCACGGTTATTTTGGCCGA
ACTIN1	TGCGACAATGGAACTGGAATG	GGATAGCATGTGGAAGTGCATACC
atpB	TGAGAACAAATCCTACTACTTC	TTTTCCCCCACGACGATAAG
rps18	GAATAAATCTAAGCGACTTTTTAC	ATTTTTTTCTGGTTCTAAGACTAG
rps7	ATGTCACGCCGAGGTACTGC	AGCTCTATTTGCCTCTGCCA
	RNA stability assay	
rrn23	TTCAAACGAGGAAAGGCTTACGG	AGGAGAGCACTCATCTTGGG
psbCD	ATAACATCAAAATCTATAACATTAAGG	GTTGGATGAATCTATTTTTCTC
psbC	ATGAAAACCTTATATTCCCTGAG	TTAGTTAAGAGGAGTCATGG

Primer sequences are provided in 5‘ to 3‘ orientation.